NUMERICAL SIMULATION OF THE PERFORMANCE OF AEROBATIC AIRCRAFT

Gábor Csapó
Aero/Space Department
Berlin University of Technology
Germany

Abstract

Aircraft designed for aerobatic flight have very strong demands concerning performance, handling quality and maneuverability, due to the highly complex maneuvers which have to be executed. Describing the performance by using steady state values does not reflect the pilots impression comparing different types of aerobatic aircraft. The differences are much larger then expected when looking at values based on a standard of comparison related to steady state values. Simulation of the longitudinal dynamics is an approach of creating a tool which enables the investigation of a design concerning its capability of performing aerobatical maneuvers before actually building the aircraft. Furthermore the knowledge of the proceeding of flight dynamical parameters and of how to operate the controls during a maneuver gives the pilot an aid which helps fitting a program into the capability of the aircraft. Results of simulation show a significant impact of relatively small variations of design parameters on the aerobatic quality. This result correlates with the practical experience evaluated in numerous aerobatic flights.

1. Introduction

In order to create an instrument which makes possible the determination of the specific attributes of an aircraft regarding the performance during aerobatic flight, a simulation of the longitudinal dynamics is made. Based on a universally valid aerodynamical modeling the variation of fundamental design parameters is investigated and discussed. Exemplarily two different layouts are compared to give an impression of the influence of design improvement. The aircraft's capability to perform the following figures is considered as representative to define a basis of comparison: -Pull into vertical flightpath, -Half-loop, -Loop and Vertical climb.
The equations of motion are solved by Euler-integration. The elevator angle is governed and the flightpath is stabilized by a calculated desired radius. In this way any selected flightpath fitting into the envelope of the examined layout can be simulated. The calculation of the desired radius takes advantage of the fact that the change of airspeed during a maneuver is a slowly varying parameter compared to the short period oscillation mode.

2. General Aspects of Aerobatic Aircraft Design

Modern high performance aerobatic aircraft are piston powered single engine airplanes, with engine power between 200 and 400 horsepowers. Empty weights are in the range between 550 and 800 kg, which results in a power to weight ratio of 2.0 to 2.5 kg/Hp. The mass of engine and propeller typically require 45% of the empty weight of the airplane. The pilot is placed relatively in the back of the fuselage to enable a good overview of the attitude of the aircraft. In order to save weight, usually non retractable taildragger type landing gear is used. Steady state performance values show stall speeds of about 25 - 30 m/s, maximum horizontal speeds in the range of 85 - 95 m/s and climb rates of typically 15 m/s.

2.1. Design Criteria

Besides performance there are also demands concerning handling qualities and other overall design criteria. These are:

- Rate of roll should be at least 360°/sec
- Handling quality during spin
- Stick force gradients should be at optimum

- No coupling between lateral and longitudinal axis
- Visibility
- Symmetrical layout of the airfoil
- Structural limit of at least +/-10g
- Handling quality during flick maneuvers
- No buffeting during rolling turns

2.2. Design Conflicts in the Layout of Aerobatic Aircraft

The overall design needs determination of major parameters where the relative optimum varies according to the flight condition. Sometimes performance considerations have to be sacrificed for handling quality. Most of all the wing layout is critical. The impact of wing aspect ratio on the quality of the aircraft is very strong.
A wing with high aspect ratio will lead to a lower induced drag which is dominant at all maneuvers with high load factors. Increasing the wing aspect ratio will result in significantly better overall aerobatic performance. The large disadvantage of a wing with a high aspect ratio is that the maximum rate of roll will be decreased and adverse yaw, which is very uncomfortable, will be enlarged.

3. Aerodynamical Modelling

Since competitional aerobatic flight is executed in a range with a maximum speed of approximately 130m/s, mach-number effects can be neglected.
Remarkable is the type of wing airfoil commonly used on newest aerobatic aircraft. Figure 1 shows the general layout. The experience made with this kind of airfoil is that the stall occurs suddenly and with a strongly developed hysteresis, so that flick maneuvers can be flown very precisely. Measurements show that there is an almost exactly linear connection between lift and angle of attack until maximum lift is reached, behind that point lift collapses abruptly. Due to this characteristic a linear approximation between lift and angle of attack is of high accuracy.

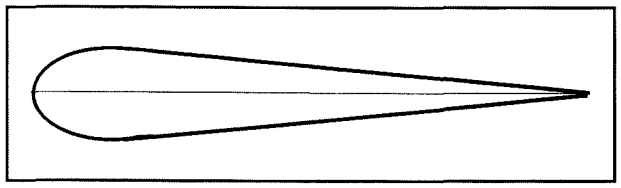

FIGURE 1: Wing airfoil commonly used on modern high performance aerobatic aircraft. Elliptical front section with straight tailcone

3.1. Wing:

Lift forces of the wing can be determined by:

$$F_{LW} = \frac{\rho}{2} v_\infty^2 A_W c_{LW} = \frac{\rho}{2} v_\infty^2 A_W c_{L\alpha W} \alpha$$

with:

$$c_{W\alpha} = \frac{\partial c_W}{\partial \alpha} = \frac{2\pi \Lambda_W}{\Lambda_W + 2}$$

Induced drag can be calculated with:

$$c_{Di} = \frac{c_L^2}{\pi \Lambda_W} k$$

Wherein k describes the enlargement of induced drag if lift distribution is different from the elliptical. If the wing is built without washout following equation is valid:

$$k \neq f(c_L)$$

The change of airfoil parasite drag with lift coefficient is taken into account by:

$$c_{Dp} = c_{D0p} + k_p c_L^2$$

Total drag of the wing is then:

$$F_{DW} = \frac{\rho}{2} v_\infty^2 A_W \left(c_{Di}(c_L) + c_{Dp}(c_L) \right)$$

3.2. Elevator:

Calculation of the elevator forces are basically made the same way as for the wing. The major extensions are that the elevator deflection angle has to be taken into account and that the elevator is influenced by the wing. Since the elevator is downstream of the wing, its downwash changes the direction of airflow on the elevator. It can be described by the expression $\partial \alpha_W / \partial \alpha$. A change of angle of pitch around the center of gravity also induces an angle of attack on the elevator which acts as a damping moment.

Elevator lift-angle of attack ratio can be determined with:

$$c_{L\alpha E} = \frac{\pi \Lambda_E}{1 + \sqrt{1 + \frac{\Lambda_E^2}{4}}}$$

A change of angle of pitch around the center of gravity induces an angle of attack on the elevator which is:

$$\alpha = \frac{q(r_E - x_N + c_{SM}|\mu)}{v_\infty}$$

Lift coefficient is then:

$$c_{AH} = c_{A\alpha H}\frac{(r_H - x_N + c_{SM}|\mu)}{v_\infty}q = c_{AqH}q$$

$$\Rightarrow c_{AqH} = c_{A\alpha H}\frac{(r_H - x_N + c_{SM}|\mu)}{v_\infty}$$

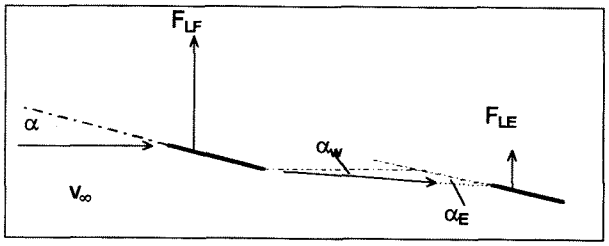

FIGURE 2: Elevator influenced by wing downwash

Lift forces on the elevator are then:

$$F_{LE} = \frac{\rho}{2}v_\infty^2 A_E\left(c_{L\alpha E}\alpha_E\left(1 - \frac{\partial_{\alpha w}}{\partial_\alpha}\right) + c_{L\eta}\eta + c_{LqE}q\right)$$

The induced drag coefficient of the elevator becomes:

$$c_{DiE} = \frac{c_{LE}^2}{\pi\Lambda_E}k = \frac{\left(c_{L\alpha E}\alpha_E\left(1 - \frac{\partial_{\alpha w}}{\partial_\alpha}\right) + c_{L\eta}\eta + c_{LqE}q\right)^2}{\pi\Lambda_E}k$$

The change of elevator airfoil parasite drag with lift coefficient is taken into account by:

$$c_{wpH} = c_{w0pH} + k_p c_{AH}^2$$

The component of lift on the elevator parallel to the aircraft´s velocity vector is

$$c_{W\alpha W} = c_{AH}\sin\alpha_W = c_{AH}\sin\left(\frac{\partial\alpha_W}{\partial\alpha}\alpha\right)$$

if $\alpha << 1$ then:

$$c_{W\alpha W} = c_{AH}\frac{\partial\alpha_W}{\partial\alpha}\alpha$$

Drag of the elevator is then:

$$F_{DE} = \frac{\rho}{2}v_\infty^2 A_E\left(c_{DP}(c_{LE}) + c_{DiH}(c_{LE}) + c_{LE}\frac{\partial\alpha_W}{\partial\alpha}\alpha\right)$$

3.3. Propeller Thrust

Propeller thrust can be determined on the basis of elementary propeller theory if the aircraft´s speed is in a range in which compressibility effect is insignificant. In this theory the propeller is modeled as a disk on which a pressure rise occurs. Behind the propeller the pressure is converted into kinetic energy, so that the stream velocity behind the disk is higher than in front of it.
Generally thrust can be calculated on the theorem of momentum by the following equation:

$$F_T = \dot{m}(v_{jet} - v_\infty)$$

For an incompressible flow it can be proved that the following relation is valid:

$$v_{Prop} = \frac{v_\infty + v_{jet}}{2}$$

massflow is:

$$\dot{m} = v_{Prop}\rho A_{Prop} = \frac{v_\infty + v_{jet}}{2}\rho A_{Prop}$$

this results in:

$$F_{Thrust} = \frac{1}{2}(v_{jet}^2 + v_\infty^2)\rho A_{Prop}$$

The power in the jet behind the propeller can be determined by energy considerations:

$$P_{jet} = \frac{1}{2}\dot{m}(v_{jet}^2 - v_\infty^2)$$

so that:

$$P_{jet} = \frac{1}{2}\rho A_{Prop}(v_\infty + v_{jet})(v_{jet}^2 - v_\infty^2)$$

With this equation the velocity of the jet behind the propeller can be determined and with that propeller thrust can be calculated. Propeller efficiency is defined the following way appropriately:

$$P_{jet} = P_{Engine}\cdot\eta_{prop}$$

4. Simulation

The differential equation in the body axes system of coordinates of longitudinal motion is:

$$m(\dot{u}_b + w_b q) = -mg \cdot \sin\Theta + X_b$$

$$m(\dot{w}_b + u_b q) = mg \cdot \cos\Theta + Z_b$$

$$I_y \dot{q} = M_y$$

$$q = \dot{\Theta}$$

This equation can be solved by numerical integration after transforming the aerodynamical forces into the body axes of coordinates. Euler type integration was used to shorten the time constants for the governor.
The determination of the position relative to the earth can be made after transformation into the geodatical system of coordinates by:

$$x_b = \int \dot{x} dt = \int u_g dt$$

$$z_b = \int \dot{z}_g t = \int w_g dt$$

Angle of attack and velocity can be calculated in the body axes system of coordinates by:

$$\alpha = \arctan\left(\frac{w_b}{u_b}\right)$$

$$V_\infty = \sqrt{u_b^2 + w_b^2}$$

The radius of flightpath can be determined by knowledge of velocity, loadfactor and angle of flightpath:

$$R = \frac{mv^2}{F_L - mg\cos\gamma} = \frac{v^2}{n - g\cos\gamma}$$

The application of a closed control loop system as described in figure 3 governs the radius of the flightpath. Nevertheless the cyclical deviations accumulate in a way that the flightpath is drifting away downwards. The resulting flightpath has similarity to the one shown in figure 6, although the altitude loss during one cycle is much smaller. Because of this potential energy is converted into kinetic energy.

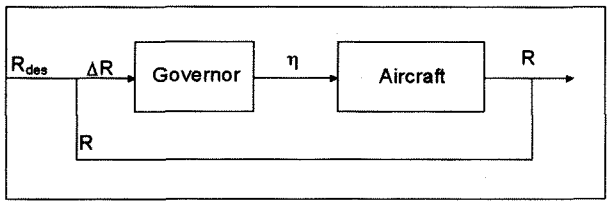

FIGURE 3: Closed control loop system

This problem can be solved by calculating a desired radius with which the flightpath is stabilized. It appears that both the information of the present distance to the intended position as well as the angle of flightpath have to be taken into account. After several tries the determination of the desired radius according to geometrical considerations as described in figure 4 has proved to be fully satisfactory. The path converges very well into the intended.

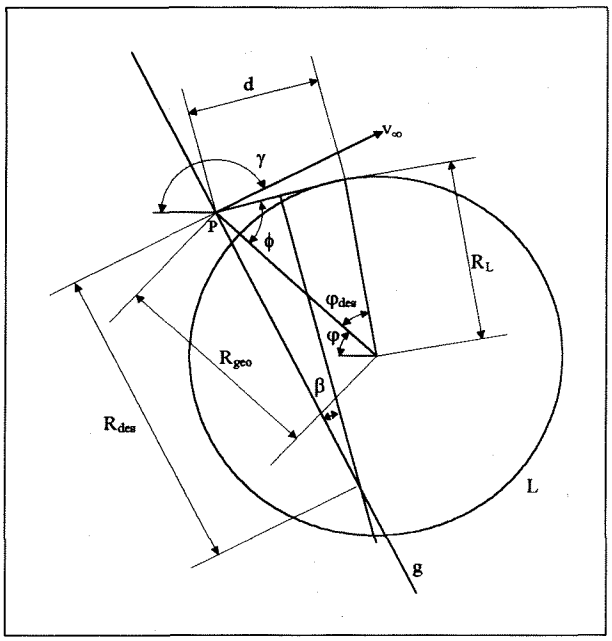

FIGURE 4: Geometrical considerations to the calculation of the desired flightpath radius

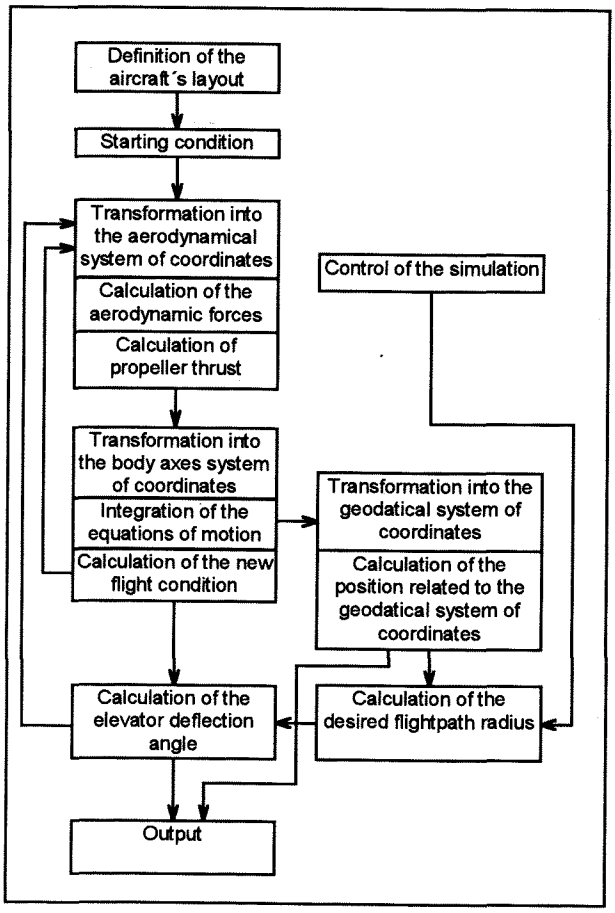

FIGURE 5: Process of simulation

5. Results

Figures 6 and 7 show the quantitative form of flightpathes resulting when the elevator angle is held constant. In this (more theoretical) case the fundamental form of the line is greatly influenced by the location of center of gravity. A large amount of static stability (forward center of gravity location) will lead to a form shown in figure 6. In contrast figure 7 demonstrates the situation if center of gravity and neutral point are in the same point. In the first case form of the path is like a cycloid, angle of attack varies only a little during a period of one loop however radius of flight path varies periodically. At the upper half the turn is lightened, in the lower half a larger radius is flown. In the second case the periodical changes of radius are small but changes of angle of attack can be observed.

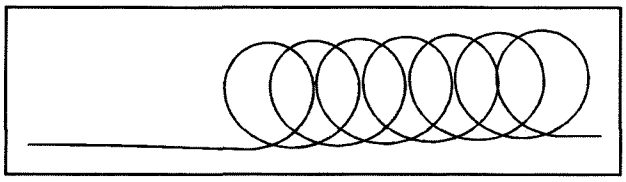

FIGURE 6: Flightpath resulting with elevator deflection angle held constant. 20% static stability.

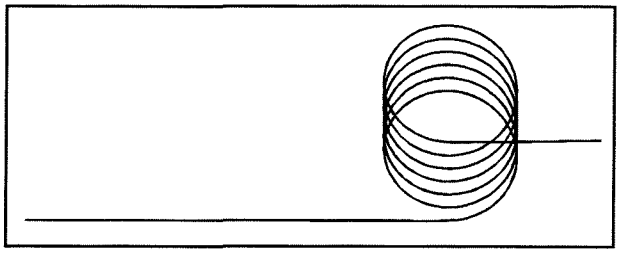

FIGURE 7: Flightpath resulting with elevator deflection angle held constant. Center of gravity in neutral point

It can be found that elevator deflection angle dictates an angle of attack when the center of gravity is in a forward location. In an rearward center of gravity position elevator angle dictates more a radius. This conclusion can not be used for performance description but it is of great importance to the piloting technique. When flying an airplane with a high amount of static stability stick movements during a maneuver have to be made larger than in an airplane with low static stability to obtain a flight path of constant radius. Flying figures with a constant radius is important to achieve high scores on the figures during contests.

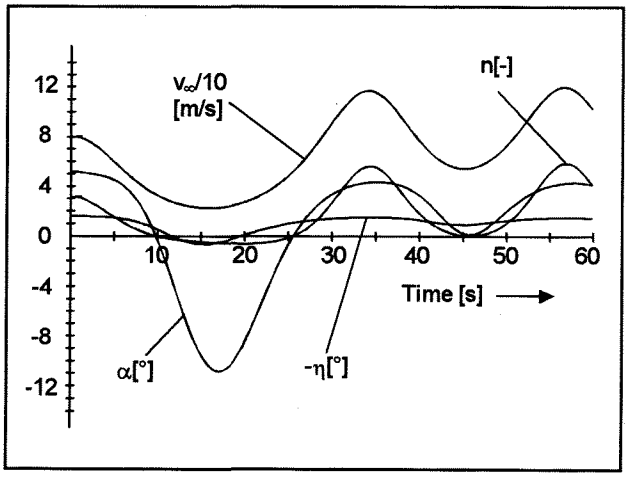

FIGURE 8: Course of parameters during the execution of a circular loop

Figure 8 shows the time history of flight dynamical parameters as well as the required elevator deflection angle for an aircraft as defined by configuration 1 (table 1) flying a cicular loop with a radius of 300m. Entry speed is 80m/s.
In order to demonstrate the effect of varying aircraft layout two different designs are compared wherein aircraft (1) represents the EXTRA 300, today's most commonly flown design and aircraft (2) an improvement by enlarging aspect ratio from 6.0 to 7.0 and engine power by 10% as well as reducing weight by 70 kg. These changes are values which can be assumed as realistic in the next future by using more advanced building technique and materials. Table 1 shows the parameters which represent these two compared designs.

Configuration		1	2
Mass	[kg]	800	730
Wing area	[m²]	10.7	10.0
Wing aspect ratio	[-]	6.0	7.0
Max. lift coefficient	[-]	1.3	1.3
Longitudinal stability	[-]	0.1	0.1
Elevator area	[m²]	2.5	2.5
Elevator aspect ratio	[-]	4.0	4.0
Elevator lever arm	[m]	4.0	4.0
Parasite drag	[m²]	0.28	0.25
Engine power	[KW]	220	242
Propeller diameter	[m²]	2.0	2.0
Propeller efficiency	[-]	0.89	0.89

TABLE 1: Description of the two compared design layouts

Figure 9 and 12 are velocity-load factor diagrams in which the aircraft's capability to perform loops is added according to the simulation. Line 1 is the aerodynamic border of the airplane. Load factor can not be increased because of boundary separation on the wing airfoil. Line 2 describes the equilibrium in the bottom of a loop. If a loop is entered with a condition above this line, then the aircraft will leave the figure with a lower amount of total energy than it had at the beginning and vice versa in the opposite case. Line 3 describes the minimum entry conditions. Trying to enter a loop below this line, that is equivalent to a too large radius, will cause the airplane to reach maximum lift coefficient after completion of about 150° of the figure. This means the pilot will encounter inverted stall. Usually this maneuver makes the airplane enter an inverted spin. The envelope in which loops can be performed is significantly enlarged. This means that the pilot can choose out of a much wider range of flight situations from which he can enter this figure with the consequence, that the variety of possible preceding figures is dramatically enlarged.

Figure 10 and 13 show the speed at the beginning of a vertical climb as a function of entry speed at horizontal flight for different flightpath radius.
Figure 11 and 14 show the speed after performing a half-loop as a function of entry-speed. The results here are analog as can be seen in the velocity-load factor diagram. The relatively minor improvements realized in layout 2 provide a great enlargement of the range in which aerobatic maneuvers can be performed.
The improvement is not only related to the particular figure which is concerned. A further factor is of major importance. The wider range in which an aerobatic figure can be entered enlarges the variety of figures that can follow each other dramatically. The consequence is that entirely different programs can be flown. The pilot will have to pay less attention to the operational limits of his aircraft when putting together a program. Also the improvements cause the airplane to be more forgiving during aerobatic flight. This is highly desirable during a contest, because minor mistakes in one figure can be aggravated by the following one. A more powerful airplane is of great advantage in this case.

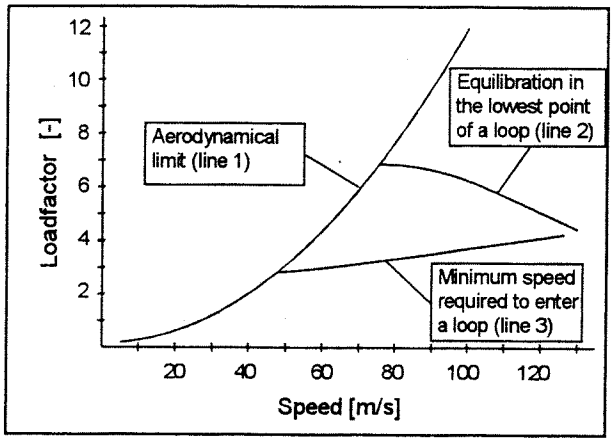

FIGURE 9: Speed-Loadfactor-Diagram including the capability to perform loops according to the results of simulation. Configuration 1

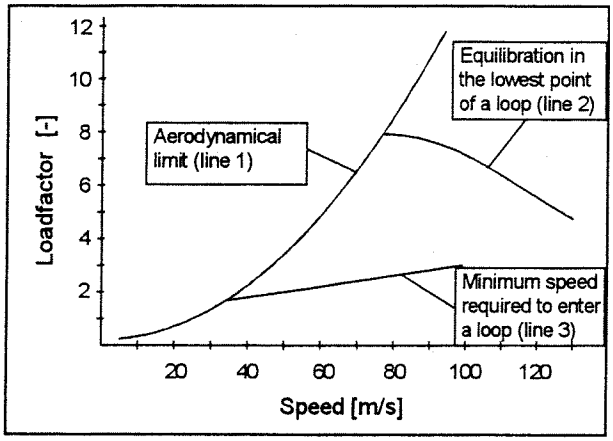

FIGURE 12: Speed-Loadfactor-Diagram including the capability to perform loops according to the results of simulation. Configuration 2

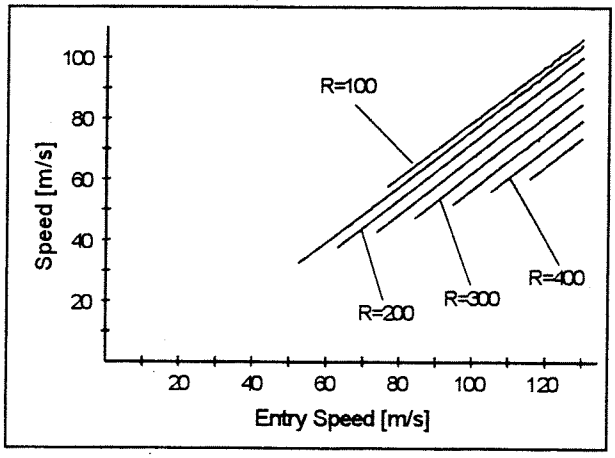

FIGURE 10: Speed after pulling into a vertical flight versus entry speed. Radius of flightpath as parameter. Configuration 1

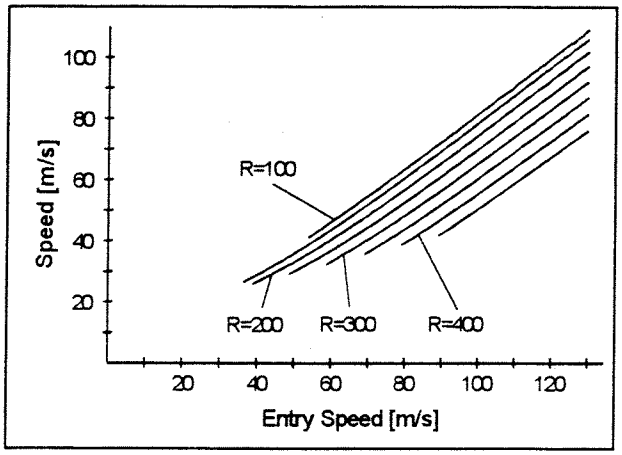

FIGURE 13: Speed after pulling into a vertical flight versus entry speed. Radius of flightpath as parameter. Configuration 2

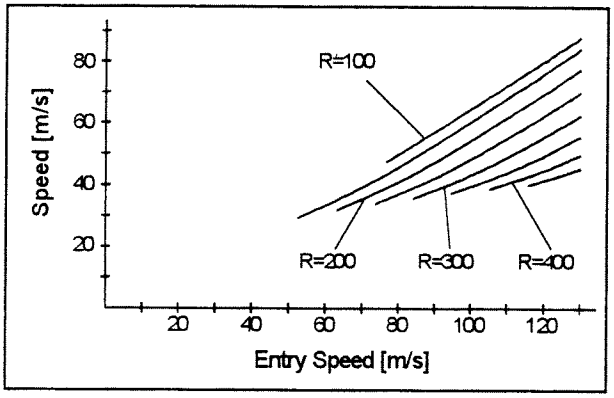

FIGURE 11: Speed after completion of a half-loop versus entry speed. Radius of flightpath as parameter. Configuration 1

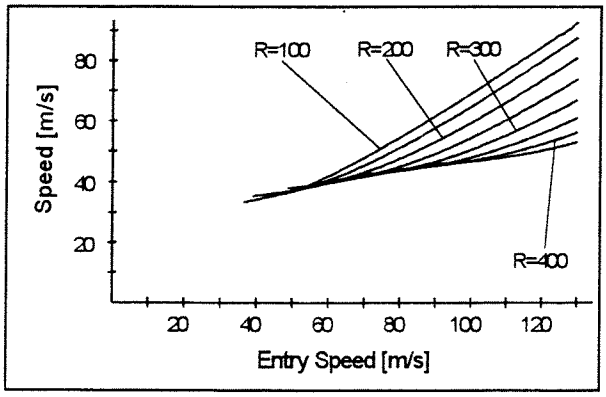

FIGURE 14: Speed after completion of a half-loop versus entry speed. Radius of flightpath as parameter. Configuration 2

6. Application for future Design

Within a certain range the layout of aerobatic aircraft can be varied. This concerns mainly wing planform (aspect ratio and taper ratio), parasite drag, tailplane configuration and power to weight ratio.
In contrast to transport aircraft, the influence of aspect ratio on the weight of the wing is not significant, so that two different aircraft with the different wing layout can be compared regard less to all other design parameters.

6.1. Wing aspect ratio: Generally an increase of wing aspect ratio will lead to better performance values, because of lower induced drag, which is very dominant at high loadfactors. On the other hand, there are disadvantages, which have to be considered : Adverse yaw will be enlarged and rate of roll will be reduced. Simulation gives the designer the knowledge he needs to be able to decide how much performance loss can be accepted in order to improve maneuverability.

6.2. Taper ratio: The wing taper ratio is of marginal influence on the performance, however it is of great importance to the handling qualities. A tapered wing has a significantly lower adverse yaw compared to a straight wing. In addition wing bending moments are reduced. Lift distribution is influenced in a way that the local lift coefficient is enlarged at the outer part of the wing. Accordingly stall characteristic is less forgiving, but this is compensated by pilot skill. Because of these reasons common aerobatic aircraft have taper ratios of about 2:1.

6.3. Parasite drag: Naturally minimization of parasite drag is a main goal in each aircraft design. On the other hand it is important to find the proper compromise between drag and weight. By installing a retractable landing gear for example, parasite drag can be decreased significantly, but saving the additional weight of the installation is a strong argument and simulation results show that in this case it is more useful to save extra weight, than to reduce drag. This relationship could change if it was possible to build a relatively light weight retractable landing gear system and if average speeds at which the airplane flies were enlarged.

6.4. Tailplane configuration: There is only a neglectable impact of the tailplane configuration on the aerobatic performance of a design. Therefore handling quality and maneuverability criteria are the fundamental basis for tailplane design.

6.5. Power to weight ratio: This parameter has proved to have the most significant impact on the performance of aerobatic airplanes. An improvement in power to weight ratio will cause the airplane to perform severely better, without creating any disadvantages.

In order to improve the aerobatic capability of an aircraft, it is most important to make the overall design as light weight as possible. Since the power to weight ratio is of largest impact there is a difference between improving this value by reducing weight or by enlarging engine power. While the latest does not have a negative influence on handling qualities, it also does not provide any improvement. However there are two benefits that can be achieved by reducing weight. The obvious one is improving power to weight ratio. On the other hand, a lighter airplane can be built with a proportionally smaller wing, if wing loading is held constant.
The result of decreasing wing area at a constant wing span is that wing aspect ratio will be enlarged resulting in a secondary improvement. Wing aspect ratio can be enlarged without obtaining negative effects on rate of roll by reducing wing area only. Thus wing loading is determined by the required stall speed and maximum lift coefficient of the airfoil so that this is a factor where large variations can not be made.

6.6. Concluding Remarks:

The aerodynamical modeling was made in a relatively simple manner to allow the investigation of the general influence of design parameters rather then to determine the exact performance of one particular aircraft. Principally this task can be solved as well it would only require a precise description of the aircraft's aerodynamics. The results of the calculation show a large similarity to the experience evaluated in several aerobatic flights and show that this approach leads to a useful additional tool when developing of an aerobatic aircraft. Besides performance also more subjective impressions of the pilot are also of major concern, and a designer needs experience to be able to interpret the simulation results.

The most important general question that has to be raised is what happens and how large is the impact when the aircraft is not flying an ideal shaped flight path, so as that a loop is not an exact circle or an

immelmann is not a precisely flown half loop. In these cases energy transformation is changed. For example during an immelmann a pilot can recover the maneuver after beginning with a too low speed by tightening the flightpath in the upper part of the half loop and consequently achieving a higher entry speed for the following roll. The problem of answering these questions is not a problem of simulation technique but rather of interpreting the results.

7. References.

(1) Brockhaus;
Flugregelung

(2) Brüning,G./Hafer,X.;
Flugleistungen, Springer Verlag, Berlin-Heidelberg-New York 1978

(3) Csapó,G.;
Entwicklung eines numerischen Verfahrens zur Beschreibung und Bewertung der Flugleistungen von Kunstflug-Flugzeugen.
Diplomarbeit, TU Berlin 1995

(4) Etkin,B.;
Flugmechanik und Flugregelung,
Berliner Union, Stuttgart 1966

(5) Federation Aeronautique Internationale,
Aerobatic Catalogue, Adopted by the FAI Aerobatics Commission (CIVA),
1987

(6) Föllinger,O.;
Regelungstechnik, Elitera-Verlag,
Berlin 1978

(7) Fuchs,T.;
Flugleistungs- und Flugeigenschafts-untersuchungen an einem modernen Motorkunstflugzeug, Diplomarbeit,
TU Braunschweig 1985

(8) Giencke,E.;
Einführung in die Flugmechanik,
Vorlesungsskriptum, TU Berlin

(9) Münzberg,W.;
Flugantriebe, Springer Verlag,
Berlin-Heidelberg-New York 1972

(10) Rosenberg,R.E.;
Flugleistungserprobung von Strahlflugzeugen.Grundlagen-Versuchsablauf-Versuchsauswertung, Springer Verlag, Berlin-Heidelberg-New York-London-Tokyo 1987

(11) Schlichting,H./Truckenbrodt,E.;
Aerodynamik des Flugzeugs, Bd. 2
Springer Verlag, Berlin-Heidelberg-New York 1969

(12) Thomas,B.;
Fly for Fun, Edited by:
Foley,H./Thomas,J. 1985

(13) Thomas,B.;
Fly for Fun to Win, Edited by:
Thomas,J./Privateer,G. 1987

(14) Wagner,A.;
Handbuch des Kunstflugs,
Luftfahrt-Verlag Walter Zuerl 1973

(15) Williams,N.;
Loopings and Turns, Motorbuchverlag

(17) Military Specification: Flying Qualities of Piloted Airplanes, MIL-F-8785 b, 1965